

NOAA AVHRR derived Aerosol Optical Depth over Land

A. Hauser, D. Oesch, N. Foppa and S. Wunderle

Institute of Geography, University of Berne, Switzerland

**Accepted for publication in Journal of Geophysical Research -
Atmospheres.**

Copyright 2005 American Geophysical Union.

Further reproduction or electronic distribution is not permitted.

A. Hauser, Institute of Geography, University of Berne, Hallerstr. 12, 3011 Berne, Switzerland
(adrian@giub.unibe.ch)

Abstract. Aerosol optical depth was retrieved from a time series of NOAA-16 AVHRR data from May 2001 through December 2002 for Central Europe (40.5°N-50.0°N, 0°E-17°E). In contrast to classical methods, no a priori knowledge of the surface reflectance is necessary but instead the surface reflectance is estimated from a time series including the previous 44 days. Additionally, the area where aerosol optical depth can be retrieved is no longer limited to certain land cover types. Only bright surface targets are excluded in the retrieval. To retrieve the aerosol optical depth, the radiative transfer code SMAC is used. Afterwards the data is averaged within a 25×25 pixel region to increase the retrieval precision. The resulting standard deviation of the aerosol optical depth within this region is used as a quality control parameter and suitable for a post-processing of the initial aerosol retrieval. This post-processing leads to a substantial increase in the retrieval accuracy when compared to ground-based AERONET measurements. Over 650 co-incident AVHRR retrievals and AERONET measurements were compared and a correlation coefficient of 0.70 was found. Altogether, the proposed method offers the potential to generate an aerosol climatology based on NOAA AVHRR data, which dates back to the early 1980s.

1. Introduction

The reports of the Intergovernmental Panel on Climate Change in 1995 and 2001 [*IPCC*, 1995, 2001] have drawn lots of attention to aerosol related research. As stated in the reports, there are large uncertainties concerning both, the direct and indirect effects of aerosols and the level of scientific understanding is low. Ground-based aerosol measurements cannot assess global trends of the aerosol budget because of the short lifetime of aerosols and the resulting strong spatial variations in the aerosol concentration. However, they remain indispensable for validation of air borne or space borne remote sensing sensors. The MODerate resolution Imaging Spectroradiometer (MODIS) on board Terra and Aqua and the Multiangle Imaging Spectroradiometer (MISR) on board Terra have provided new insights into aerosol physics. Besides a better understanding of the physical and chemical basics of aerosols, it is also of great interest to monitor temporal aerosol trends. Aerosol time series of twenty or more years are only derivable from Total Ozone Mapping Spectrometer (TOMS) measurements and from the Advanced Very High Resolution Radiometer (AVHRR). The majority of AVHRR aerosol research is directed towards the retrieval of aerosol information over oceans, e.g. by *Stowe et al.* [1997], *Husar et al.* [1997], *Mishchenko et al.* [1999] and *Geogdzhayev et al.* [2002]. Oceans cover not only about 70% of the Earth's surface but have some characteristics, which make them favorable for aerosol research: First, the ocean has a low, spectrally flat surface reflectance, which is spatially invariant. Second, the bidirectional reflectance distribution function (BRDF) of sea water is well-known. Even though, white caps and chlorophyll might lead to substantially higher reflectances in some cases. Altogether, the ocean surface signal is

rather low providing a high sensitivity to the aerosol signal. Using these constraints, some additional information about aerosols have been retrieved, e.g. the aerosol size [*Higurashi et al.*, 1999; *Mishchenko et al.*, 1999]. The only operational aerosol product from AVHRR is provided by the National Oceanic and Atmospheric Administration (NOAA) [*Ignatov et al.*, 1995; *Stowe et al.*, 1997; *Ignatov et al.*, 2004].

Land surfaces have compared to ocean surfaces several disadvantages: The surface reflectance is neither homogeneous nor temporally stable. Most bidirectional distribution function (BRDF) models require information about the land cover, which is difficult to retrieve and often outdated. The surface reflectance of land compared to oceans is generally higher and leads to a reduced sensitivity to aerosols combined with larger uncertainties concerning the surface reflectance and the bidirectional component. Therefore, only few studies dealing with the retrieval of aerosols over land using NOAA AVHRR exist so far. *King et al.* [1999] give an overview over different remote sensing techniques from AVHRR to estimate the tropospheric aerosol load. From the more recent studies dealing with AVHRR and aerosol retrievals one should especially mention the study from *Knapp and Stowe* [2002] to assess the potential of AVHRR Pathfinder data for a global aerosol climatology. *Holzer-Popp et al.* [2002a, b] propose the synergetic use of the Along Track Scanning Radiometer (ATSR-2) and the Global Ozone Monitoring Experiment (GOME) spectrometer. This potentially operational synergetic aerosol retrieval method is portable to GOME-2/AVHRR on METOP.

The most widely used concept for aerosol retrieval over land from NOAA AVHRR is the identification of dark surface target like dark dense vegetation (DDV) [*Kaufman and Sendra*, 1988; *Soufflet et al.*, 1997]. These targets exhibit a very low surface reflectance,

i.e. the signal is dominated by the contributions from the atmosphere due to scattering by molecules and aerosols. In addition, the surface reflectance variations with varying satellite zenith angles of dark targets are reduced compared to more bright targets and the sensitivity to aerosol is higher [Kaufman, 1987]. The major disadvantage of this method is that only few pixels match the requirements of dark pixels, e.g. in Europe less than 1% of the land pixels can be labeled as pure DDV pixels [Borde *et al.*, 2003]. The sparse number of DDV targets does not permit the generation of aerosol maps or an aerosol climatology. As a consequence, the application of the DDV concept for atmospheric correction of remote sensing imagery is restricted. Von Hoyningen-Huene *et al.* [2003] estimate the surface reflectance by applying a mixing model of bare soil and green vegetation spectra, tuned by the Normalized Difference Vegetation Index (NDVI). However, the NDVI itself is not independent of the aerosol load and might lead to an inaccurate surface reflectance. The problem of the directional nature of the surface reflectance is addressed by Borde *and Verdebout* [2003]. The surface reflectance is retrieved at AERONET stations but this limits the application to very few pixels.

After a brief summary of the data and the processing (chapter 2), we present a method to estimate the surface reflectance over land, which accounts for the bidirectional reflectance signal, independent of the surface cover (section 3.1). Afterwards, we spend a few thoughts on the implications arising from the surface reflectance estimation (section 3.2). The aerosol optical depth retrievals are then validated using data from ground-based sun photometers from various sites of the Aerosol Robotic Network (section 3.3) and the results are presented (section 3.4). Then, we briefly discuss the applicability of the pro-

posed method to water bodies (section 3.5). Chapter 4 contains a discussion of possible error sources. Conclusions are drawn in chapter 5.

2. Dataset summary

2.1. AERONET data

AERONET (AErosol RObotic NETwork) is a federation of ground-based remote sensing instruments measuring aerosol and its characteristics. The network imposes standardization of instruments, calibration and processing. The highest level product, the level 2.0 (cloud-screened and quality-assured), was used in this study and the expected accuracy of the aerosol optical depth is about 0.02 [Holben *et al.*, 1998]. In the period May 2001 till December 2002 level 2.0 data has been available for eleven AERONET sites [Table 1], however, the number of measurements per site varies substantially. In order to compare AERONET and AVHRR retrieved aerosol optical depth, the AERONET optical thickness has to be determined for the wavelength of $0.55\mu\text{m}$. First- and second-order interpolation schemes are reported in the literature [Ångström, 1961; King *et al.*, 1980] but differences between both schemes were statistically not significant. Like most other studies comparing satellite retrieved aerosol optical depth with ground-based measurements, we continue to use a second-order polynomial fit in logarithm of wavelength [Ignatov *et al.*, 1995; Stowe *et al.*, 1997; Knapp and Stowe, 2002].

The AERONET site of Venice marks a special case. Even though the station name suggests a continental site, it is actually located 15 kilometers off Venice in the Adriatic Sea. Venice is excluded in the validation of the surface reflectance estimate but used in the validation of the aerosol optical depth because it offers a large and well maintained amount of data.

2.2. NOAA AVHRR data

The University of Bern (46.93°N / 7.41°E) is ingesting NOAA AVHRR data since the 1980s. The data presented in this paper uses observations from the six channel AVHRR/3 instrument on board the polar orbiting NOAA-16 satellite. The AVHRR measures emitted and reflected radiances in the following bands: 0.58-0.69 μm (channel 1), 0.70-1.01 μm (channel 2), 1.57-1.64 μm (channel 3A), 3.49-4.04 μm (channel 3B), 10.10-11.77 μm (channel 4), and 11.40-12.70 μm (channel 5). The nominal instrument spatial resolution at nadir is 1.1 km. The ‘morning’ satellites are typically in an orbit with a local equator crossing time (EXT) in early morning (EXT \sim 07:30 and \sim 19:30) while the ‘afternoon’ satellites pass on the local afternoon (EXT \sim 13:30 and \sim 01:30). For aerosol retrievals, the illumination conditions are more favorable for the afternoon passes. Due to data quality issues and availability of both, AVHRR and AERONET data, the dataset consists of the NOAA-16 afternoon passes from May 2001 through end of December 2002. With respect to other remote sensing activities focussing on the Alps, our region of interest is limited to an area covering Central Europe from 40.5°N to 50°N and 0°E to 17°E. The primary tasks of the AVHRR were qualitative applications such as cloud detection, so no on board calibration facility was provided. However, these channels have since found wide ranging applications far exceeding design expectation. With its extensive data archive dating back to the early 1980s, it is a very interesting sensor for long-term monitoring of various parameters. The goal of change detection over decadal timescales requires precise knowledge of sensor calibration spanning several different instruments. Otherwise apparent changes might be falsely assigned to the surface instead to sensor drift.

Up to 2003, there are no continuously updated post-launch calibration coefficients available for NOAA-16. The NOAA National Environmental Satellite Data and Information Service (NESDIS) started this service in 2003. The calibration method using space count coefficients [Mitchell, 1999, 2001] has been chosen with regard to intercalibration of several AVHRR instruments, an important issue for other remote sensing activities of our working group. In principle, the space count should remain invariant at a nominal value near 40 counts throughout the life of the instrument. However, small variations of the order 0.5 count have been observed. Although inconsequential for most applications, these variations are significant for dark target applications such as retrieval of aerosol optical depth over the ocean. The thermal channels 4 and 5 of the AVHRR/3 are calibrated according to Section 7.1.2.4 of the NOAA-KLM user's guide [Goodrum *et al.*, 2000]. The performance of the cloud masking process depends to a great extent on correct brightness temperatures of the thermal channels.

Accurate georeferencing is another vitally important step in pre-processing. In addition to a precise external time, we used a feature matching algorithm to achieve sub-pixel accuracy. The rectification process is carried out by using piecewise linear mapping functions throughout the whole image. Input and output images are partitioned into patches defined by closest grid points. An affine transformation function is evaluated at every pixel on the output image by using three closest georeferenced points on the grid and their respective image coordinates.

The Alps and other mountainous regions like the Apennine and the Pyrenees are present in our images and require some consideration. An orthorectification algorithm has been applied to avoid displacement errors introduced by the topography. One of the most

important steps in the retrieval of aerosols is a proper cloud masking. Otherwise an increase of the surface reflectance due to cloud contamination will be wrongly interpreted as an aerosol signal. The Cloud and Surface Parameter Retrieval (CASPR) system is a toolkit tailored for the analysis of AVHRR data [Key, 2002]. The advantage of the CASPR package is its strength in discriminating between clouds and a snow covered surface. The algorithm quality has been proofed by *Di Vittorio and Emery* [2002]. Additionally, an algorithm based on *Simpson and Stitt* [1998] to flag cloud shadows has been incorporated.

3. Aerosol retrieval from NOAA AVHRR data

3.1. Surface Reflectance of Channel 1 ($0.63\mu\text{m}$)

The difference between the measured top of atmosphere reflectance and the estimated surface reflectance is directly related to the aerosol content of the atmosphere and, to all smaller extend, to ozone and water vapor. Obviously, the quality of the surface reflectance is a very critical parameter for the aerosol retrieval. To omit errors introduced by an inaccurate BRDF model we try to determine the bidirectional component from a time series of observation. We assume that the surface target remains radiometrically invariant over a certain time period and that some of the observations are made under aerosol-free conditions. Furthermore, the aerosol-free observations are expected to be made under different satellite zenith angles. The time period in this study has been set to 45 days. A shorter time period is desirable to account e.g. for vegetation changes but is mainly limited by cloud cover. Besides the generally higher amount of cloud cover in wintertime, mountainous regions are often covered in clouds due to orographically induced condensation and blocking effects. The identification of the aerosol-free data points is done using the concept of the convex hull. The convex hull of a set of points on a single plane is

defined as the smallest convex polygon that encloses these points. To identify the polygon points, a Delaunay triangulation algorithm has been used. An example is shown in figure 1 for the AVHRR pixel covering the AERONET site of Ispra, Italy. It shows the expected run of the curve, more flat in the forward scattering direction (positive satellite zenith angles) and a sharper increase of the reflectance with decreasing satellite zenith angle in the backward scattering direction. The application of a convex hull holds the risk of emphasizing a single data point with a too low reflectance. The most important physical phenomena causing a low reflectance is cloud shadow, which has been already excluded in the pre-processing.

To get some hints about the quality, we use the aerosol and water vapor measurements of the AERONET sites and correct the AVHRR measured top of atmosphere reflectance using the radiation transfer code 6S [Vermote *et al.*, 1997]. 6S models the surface reflectance with an accuracy better than a few 1×10^{-4} [reflectance units]. Only water vapor and aerosol optical depth from AERONET stations are used, detailed simultaneous aerosol type information is sparse and therefore not considered. It is assumed that the aerosol type is continental. Starting with AVHRR top of atmosphere data, we first use the time series of observation to identify the convex hull representing the aerosol-free top of atmosphere observation. The aerosol-free top of atmosphere reflectance for the specific satellite zenith angle is then corrected for the water vapor and ozone influence and the Rayleigh optical depth, which depends on the surface pressure, i.e. basically on altitude. This correction is in line with the normal retrieval scheme for AVHRR and is performed using the SMAC algorithm and water vapor data from MeteoSwiss' Alpine Model (aLMo) and ozone data from the NCEP analysis. Through this correction, we receive a surface

reflectance for aerosol-free condition corrected for ozone, water vapor and Rayleigh scattering. This data is presented in figure 2 on the y-axis. The x-axis data is based on the same initial dataset but for the retrieval of the surface reflectance AERONET aerosol optical depth and water vapor, NCEP ozone data and the radiative transfer code 6S are used. This means that the x-axis shows the surface reflectance based on the most accurate information available while the y-axis shows the results of the proposed method. The scatter diagram (figure 2) shows in general a good correlation. The vast majority of the data points are below the 1:1 line, i.e. the surface reflectance extracted using the convex hull is generally lower than the ‘true’ surface reflectance using AERONET data and 6S. Data significantly above the 1:1 line have been mostly acquired under satellite zenith angles exceeding $\pm 50^\circ$ degrees (figure 3). For satellite zenith angles in the range between $\pm 40^\circ$, only very few data points are negative, i.e. the surface reflectance from the convex hull exceeds the modeled value. Between $\pm 40^\circ - \pm 50^\circ$, there is a moderate increase in the number of negative data points as well as a decrease in the surface reflectance difference. Exceeding $\pm 50^\circ$, the errors increase substantially. Large positive surface reflectance differences are likely to be caused by cloud and/or snow contamination. Altogether, the bidirectional signal has been reduced to a great extent, especially in the range between $\pm 40^\circ$. Figure 3 illustrates that a restriction to positive satellite zenith angles (forward scattering) is obsolete. This method works equally well for both scattering directions.

The use of a time series of AVHRR imagery to extract the surface reflectance is based on the assumption of an invariant surface reflectance. This is obviously a strong simplification, especially in spring, during the greening of the vegetation, the surface reflectance is expected to decrease and vice versa in fall. The time series of the surface reflectance

difference is plotted in figure 4. During wintertime positive deviations, caused by partial snow or cloud contamination, seems to occur more frequently. Apart from this feature, none of the sites exhibit any other kind of seasonal behavior. This supports the assumption that even such a long time period as 45 days can be used to extract a meaningful surface reflectance estimate.

As mentioned above, most studies dealing with the retrieval of aerosols from NOAA AVHRR use a priori knowledge of the surface reflectance. The estimated surface reflectance is therefore not directly comparable with other aerosol studies using AVHRR data. On the other hand, the MODIS aerosol product uses also a surface reflectance estimate, which is the basis for the retrieval of aerosol optical depth in a similar way as in this study. The MODIS aerosol product over land determines the surface reflectance by assuming a linear correlation between the $2.16\mu\text{m}$ channel and the blue ($0.49\mu\text{m}$) and red ($0.66\mu\text{m}$) channels [Kaufman *et al.*, 1997b; Remer *et al.*, 2001]. In the absence of desert dust particles, the $2.16\mu\text{m}$ channel is assumed to be undisturbed by aerosols. Being aware that both methods are not directly comparable, an attempt is still undertaken. The surface reflectance error in the red ($0.66\mu\text{m}$) channel is continuously increasing with increasing $2.16\mu\text{m}$ reflectance. Figure 2 indicates that this finding applies to AVHRR as well, we also experience an increasing error with increasing surface reflectance. The standard error of 0.011 for all AERONET sites (figure 2) is in the same order of magnitude as the surface reflectance of the MODIS product.

3.2. Implications for further aerosol retrievals

Before starting with the retrieval we spend a few thoughts on the implications we obtain from the surface reflectance estimate from figure 2. The good correlation between the

modeled data and the surface reflectance estimate using the convex hull is an indicator that this method is a robust and reliable way to determine the surface reflectance. Another important fact is that the vast majority of the data points is below the 1:1 line, i.e. the estimated value is too low compared to the modeled value. As a consequence, we must expect in the following aerosol retrieval an overestimated aerosol optical depth. Additionally, the difference between the estimated and modeled surface reflectance is increasing with increasing surface reflectance. The surface reflectance estimate is about 15-20% too low. This offers two possibilities for the further processing: First, we correct the surface reflectance estimate according to figure 2 by about 15-20%. Second, we use the initial surface reflectance estimate and correct the aerosol optical depth afterwards. To decide on which option to choose, we should consider that the aerosol optical depth, unlike the surface reflectance, is not an independent variable. This is meant in a sense that the aerosol optical depth of neighboring pixels is linked, while this is not the case for the surface reflectance. Within a certain region, we expect a more or less stable aerosol load, even though, the surface reflectance of the individual pixels might vary substantially. Thus, the performance of a correction of the surface reflectance, unlike the aerosol retrievals, can not be verified. Correcting the aerosol retrievals seems more straightforward than correcting the surface reflectance. Another advantage of an aerosol retrieval correction is that a processing procedure similar to the MODIS aerosol retrievals [*Kaufman et al.*, 1997a; *Chu et al.*, 2002] can be applied. The surface reflectance remains uncorrected and spatial averaging within a 25×25 pixel region is applied using the 10-40 lowest percentile of the retrieved aerosol optical depth. As already discussed, we can assume that the surface reflectance of the 10-40 percentile is lower than the true surface reflectance but still

remains close to the 1:1 line, i.e. we expect an overestimated aerosol optical depth, which should be still close to the true value. As a side product from spatial averaging we get the regional standard deviation of the aerosol optical depth. This parameter can be regarded as a quality indicator. A low standard deviation suggests little variation of aerosol optical depth and is a measure of the confidence of the retrieval. However, with increasing surface reflectance we must expect larger deviations from the true surface reflectance and larger aerosol variations. This will lead to an increasing standard deviation of the aerosol optical depth inside a 25×25 pixel region with increasing surface reflectance. To summarize these last thoughts: The regional standard deviation of the aerosol optical depth is expected to show a correlation with the aerosol difference from AERONET measurements and AVHRR retrievals. With increasing standard deviation we expect an increasing difference of ground-based versus satellite-based measurements, i.e. an increasing overestimation of the AVHRR retrievals compared to AERONET data. As a consequence, the regional standard deviation of the aerosol optical depth can be used in two different ways: First, we set a threshold of the standard deviation and retrievals exceeding this threshold will be rejected. Second, we apply a post-processing depending on the correlation found between the aerosol difference and standard deviation. In the following section we will retrieve the aerosol optical depth from the initial surface reflectance estimate, discuss the resulting spatial aerosol standard deviation and will then investigate the possibilities of a post-processing.

3.3. Aerosol Retrieval and Validation Approach

Once the surface reflectance is known and a few assumptions concerning the characteristics of aerosols are made, the retrieval of aerosol optical depth using a radiative

transfer model is possible. The radiative transfer code used is the Simplified Method for Atmospheric Correction (SMAC) [Rahman and Dedieu, 1994]. This code is originally a simplified version of the 5S code [Tanré *et al.*, 1990] but has been updated to 6S [Vermote *et al.*, 1997]. The advantage of SMAC is that it is easily applicable to larger data volumes without using a look-up table. Channel 1 ($0.63\mu\text{m}$) is significantly affected by variable ozone and water vapor absorption. The accuracy of the aerosol retrieval can be improved by using ozone and water vapor from ancillary sources: Ozone data is provided by the National Center for Environmental Prediction (NCEP) $1^\circ \times 1^\circ$ analysis, water vapor data from MeteoSwiss' Alpine Model (aLMo). To account for the topography, the surface pressure at the pixel level is estimated from atmospheric pressure fields at sea level from aLMo and from the GTOPO30 digital terrain model. Aerosol retrieval from a single channel AVHRR algorithm requires a priori knowledge of aerosol characteristics. For Central Europe, a continental aerosol model [D'Almeida *et al.*, 1991; Kaufman *et al.*, 1997a] seems to be appropriate. The validation approach of the aerosol retrieval is consistent with the MODIS aerosol validation over land [Chu *et al.*, 2002]. At least 2 out of 5 possible AERONET measurements within ± 30 minutes of the AVHRR overpass and at least 20% valid aerosol retrievals within the 25×25 pixel region are required.

3.4. Aerosol Retrieval Results

We will discuss three plots in this section, the initial aerosol retrieval (figure 5), the spatial aerosol standard deviation (figure 6) and the post-processed aerosol retrieval (figure 7).

Scatter diagrams between satellite retrievals and ground-based AERONET measurements are commonly used and discussed in the literature [Ignatov *et al.*, 1995; Ignatov

and Stowe, 2000; Stowe *et al.*, 1997; Zhao *et al.*, 2002, 2003, 2004]. The intercept of the regression line of such a scatterplot like figure 5 and 7 should be close to zero. An offset indicates errors associated with the surface reflectance estimate and/or calibration. A slope different from unity points to errors linked with an incorrect assumption about the aerosol model. Random errors like radiometric noise, cloud contamination, snow contamination and surface reflectance variability lead to an increase of the standard error (σ). Obviously, the influence of the calibration cannot be of sufficient magnitude to cause such a large offset of the intercept as seen in figure 5. The main cause for this offset is an inaccurate surface reflectance estimate as seen in figure 2. Due to an underestimation of the surface reflectance, the aerosol optical depth in figure 5 is too high and generally above the 1:1 line. This is the result we expected and a direct implication of the surface reflectance estimate. Avignon, Ispra and the total of all data show the same problems, a high intercept and a general overestimation of the aerosol optical depth. More interesting are the resulting regional aerosol standard deviations (figure 6). There is a clear trend, with increasing standard deviation we obtain an increasing difference between the AERONET measurements and the AVHRR retrievals. A limitation of the valid retrievals to a standard deviation less than e.g. 0.05 would limit the overestimation of the aerosol optical depth from NOAA AVHRR substantially. Even such a threshold cannot exclude all obvious outliers from the further processing. Another consequence of a threshold is that lots of data will be rejected. To avoid this, the linear fit from figure 6 to post-process our initial results is used. The regional aerosol standard deviation can assess the mean aerosol deviation and this bias can be subtracted from the initial retrieval results.

To evaluate the quality of this post-processing, the dataset is split randomly into two equal datasets. The first dataset is used to estimate the linear fit like in figure 6. The results from this validation phase are then applied to the second dataset to verify the post-processing quality. Both datasets are displayed in figure 7 together with the linear fit for the verification dataset. When comparing figure 7 with figure 5, there is a clear improvement of the correlation coefficient (R). The improvements are especially obvious at Avignon, besides the considerable increase of the correlation coefficient, the intercept decreased from 0.19 to 0.01 and the trend of the regression line is much more pronounced. The random error has been cut down to about half its initial value (0.15 to 0.08). For Ispra, the improvements are mainly expressed in a substantial decrease of the intercept from 0.10 to 0.04. For the set of all AVHRR aerosol retrievals the results are very similar to the findings from Avignon. There is a remarkable reduction of the intercept from 0.14 to 0.02, the standard error has been cut down from 0.16 to 0.11 and the correlation coefficient (R) increased from 0.56 to 0.70. Normally, random errors are not associated with errors introduced by the surface reflectance but mainly with cloud contamination. However, the general interpretation of scatterplots is based on studies dealing with minor variations of the surface reflectance and is assuming a stable over- or underestimation of the surface reflectance but not such high variability.

Again, we compare these results with the validation results for the MODIS aerosol product over land [Chu *et al.*, 2002]. The intercept of the MODIS retrievals is about the same magnitude as our retrievals. The MODIS processing can account for different aerosol types as well as for fine and coarse mode aerosols. Additionally, the retrievals are limited to dark vegetated targets with a $2.16\mu\text{m}$ reflectance of less than 0.15, i.e. a

0.66 μm reflectance of less than 0.075. This is expressed in a slope closer to unity than in our AVHRR retrievals but we are aware of this limitation of the AVHRR sensor. Like the slope, the correlation is generally also better for the MODIS product. There are several explanations for this, a better signal to noise ratio, more accurate calibration and better cloud screening due to additional channels. Considering these limitations of the AVHRR sensor we can conclude that the post-processing has been successful.

3.5. Aerosol Retrievals over Oceans

The proposed procedure can be applied without any restrictions to water bodies and oceans. The resulting surface reflectance estimates for oceans are in close agreement to the theoretical values from Fresnel's formulation of the reflectivity. For nadir observations, we receive a mean surface reflectance of about 0.025 for channel 1. *Soufflet et al.* [1997] assumed a value of 0.023 for their aerosol retrievals and *Bertrand and Royer* [2004] 0.025. Increased surface reflectance due to whitecaps and/or chlorophyll is generally disregarded because of the use of a 45 day time series. The retrieval of aerosol optical depths over oceans requires identification of sun glint areas. Otherwise, the increased reflectance due to specular reflectance at the ocean's surface is interpreted as an aerosol signal. Excluding half the scan line towards the sun's direction means a too stringent condition because it would exclude about half of the ocean data. So far, a sun glint mask has not been incorporated into the processing and we therefore exclude oceans from the further processing.

4. Sources of uncertainties

Figure 2-7 show that the aerosol retrievals from AVHRR over heterogeneous land surfaces are influenced by various sources:

- Calibration and sensor noise

Ignatov [2002] summarized the calibration information from various authors. He estimates the uncertainty in the calibration slope to $\pm 5\%$ for AVHRR channel 1 but emphasizes that this estimate is for a best-case situation. For May 2001 through December 2002, there is no updated calibration information available. In such a case *Ignatov* [2002] expects larger calibration slopes in the range of 7-10% for channel 1. The effects of calibration errors are reduced in the surface reflectance estimate since this value is directly extracted from the calibrated AVHRR data and not from external or a priori knowledge. If an uncertainty of the calibration causes an increase of the top of atmosphere reflectance then this will lead also to an increase of the surface reflectance estimate. The difference between top of atmosphere reflectance and the surface reflectance will be affected to a much lesser degree than the absolute reflectance values but the data provides less sensitivity to the aerosol signal when the reflectance increases. Sensor noise might be an issue because the selection of the lowest reflectance within certain intervals of the satellite zenith angle tends to favor values with a negative noise contribution. This might induce an overestimate of the aerosol retrieval.

- Surface reflectance

The surface reflectance estimate is expected to introduce the largest errors into to aerosol retrieval. For the retrieval, several assumptions have been made about the surface targets: First, we assume a temporally stable surface reflectance. The time series of the difference

between the AVHRR retrievals and the modeled data (figure 4) shows no clear seasonal trend of the surface reflectance errors. Another problem arises from short-term reflectance variations on daily or weekly time scales e.g. triggered by precipitation or drought. According to *Betts and Ball* [1997] the magnitude of the reflectance variation is dependent on the surface cover type but to assume variations of $\pm 10\%$ of the surface reflectance seems reasonable. Negative variations of the surface reflectance have a severe impact on the convex hull because these values are selected to represent the surface reflectance for the aerosol retrieval. In other words, negative variations of the surface reflectance are the major reason for the underestimation of the retrieved surface reflectance when compared to modeled results from 6S (figure 2). The amount of scatter in figure 2 can be related to the aerosol model and the single scattering albedo herein. These two effects result together in an underestimation of the observed surface reflectance of about 15%, about 10% caused by natural reflectance variations and about 5% caused by a too high single scattering albedo. The second assumption concerns aerosol-free observation under different observation angles. Variations of the background aerosol load are not expected to influence the aerosol retrievals significantly. Most areas in Central Europe experience frequently nearly aerosol-free conditions when the aerosol optical depth is about 0.05 at $0.55\mu\text{m}$. A 20% variation of the assumed background aerosol load of about 0.05 results in variations of ± 0.01 of the aerosol optical depth. This value is well below other errors and a systematic offset of the background aerosol level is corrected in the post-processing. An exception is of course an increased background aerosol load caused by volcanic activity [*Molineaux et al.*, 1998]. Undetected cloud shadows or topography induced shadows are also influencing the quality of the surface reflectance because they lead to a decrease of

the estimate, which will result in an increase of the aerosol retrieval. The extent of these effects are difficult to quantify but affect generally only very few pixels in the imagery. Spatially inhomogeneous surfaces together with geocoding inaccuracies might also affect the retrieval accuracy. Assuming e.g. a chessboard like distribution of areas with high and low surface reflectance with a similar resolution as the AVHRR imagery, it is obvious that minor inaccuracies of the geocoding result in a varying surface reflectance. Therefore, we expect that inhomogeneous areas contribute to an increased standard deviation. This speculation is supported by figure 6. Avignon shows a clear trend, with increasing standard deviation we get an increased overestimation of the aerosol retrievals compared to the AERONET data. For Ispra, the correlation is much weaker and we expect that one explanation is the fact that Ispra lies in a very inhomogeneous region consisting of urban area, water bodies (Lago Maggiore) and vegetated area. Avignon, on the contrary, is situated in a more homogeneous agricultural region. The strength of errors associated with spatially inhomogeneous surfaces and geocoding might also experience a seasonal cycle, e.g. during summer the radiometric properties of coniferous and deciduous forests are similar but differ substantially in winter. To quantify the influence on aerosol retrieval is difficult because of the mentioned spatial and temporal changes. Altogether, it is possible to assess the surface retrieval estimate from the comparison with modeled data using 6S (figure 2) but we cannot address the uncertainties quantitative to certain sources of error.

- Retrieval uncertainties

Inaccuracies in the description of the radiative transfer, of the water vapor and ozone content of the atmosphere and the selection of an inappropriate aerosol model contribute to the retrieval uncertainties. Additionally, it is very likely that spatial and temporal

variations of the aerosol optical depth inside the 25×25 pixel region and within the time span of ± 30 minutes introduce some retrieval errors [Knapp and Stowe, 2002]. Water vapor absorption in channel 1 is small and the expected variations of the water vapor content should only lead to a decrease of less than 1% of the reflectance. Ozone absorption is more important but variations of the mean conditions by $\pm 10\%$ are expected to alter the reflectance by less than $\pm 2\%$. A more detailed analysis of the retrieval errors due to fluctuations of the ozone and water vapor concentration is given in Ignatov and Stowe [2002a] and Ignatov and Nalli [2002]. Rahman and Dedieu [1994] calculated a relative error for NOAA-9 AVHRR of 2.35% when compared to 5S [Tanré et al., 1990], after updating SMAC to 6S we expect the relative errors to be minimized and estimate the errors to less than 2%. One of the drawbacks of a single channel algorithm is that the aerosol model has to be pre-defined. A continental aerosol model is appropriate for rural regions in Central Europe but does not account sufficiently for emissions of aerosols due to industrial activities and traffic [Chu et al., 2003]. The slopes of the regression lines from figure 5 and 7 support this assumption, the slopes are clearly different from unity. Significant differences of the slope from unity are most likely caused by higher soot concentrations. A lower single scattering albedo or the application of an urban aerosol model would result in a better fit [Dubovik et al., 2000]. The used continental aerosol model is apparently not reflecting some average European atmospheric conditions but the more extreme and unlikely case of a clean atmosphere. For future applications some modifications concerning the aerosol model should be made, e.g. like in the study of Holzer-Popp et al. [2002a].

- Cloud masking

Ignatov and Stowe [2002b] stated that cloud screening is of comparable if not greater

importance for accurate remote sensing than the aerosol retrieval algorithm itself. We can confirm this statement. Especially sub-pixel cloud contamination, which result in a moderate increase of the reflectance are difficult to detect with the cloud masking algorithm. However, refinements of the cloud detection are beyond the scope of this paper.

5. Conclusion

Aerosol optical depth was retrieved from NOAA AVHRR data over Central Europe for a period of 20 months. Eleven AERONET sites were used to assess the retrieval quality. A new method to estimate a pixel-wise BRDF corrected surface reflectance using a time series of observations has been used. Compared to previous methods, it offers the advantage to significantly increase the area where aerosol retrievals are possible. Additionally, it is independent of surface type and viewing geometry, a restriction to forward scattering is obsolete. Nevertheless, satellite zenith angles in excess of ± 50 degrees showed increased errors. Besides, the method is expected to fail when applied to very bright surface targets since the sensitivity to the aerosol signal is then too low for meaningful retrievals.

The surface reflectance estimate can be applied to full resolution AVHRR imagery but the resulting underestimation of the surface reflectance requires some spatial averaging in the following processing step. The arising spatial aerosol standard deviation is a useful quality parameter, either for rejecting retrievals exceeding a certain threshold or for post-processing of the aerosol optical depth results. The post-processing increased the retrieval results significantly while reducing errors incorporated by the underestimated surface reflectance.

The pixel-wise BRDF corrected surface reflectance method is generally applicable to AVHRR-like sensors, i.e. to sensors providing a high temporal resolution. Surface cover or viewing geometry pose no restriction. This method offers the possibility to do further steps towards an aerosol climatology based on AVHRR dating back to the early 1980s. One of the major problems when building an AVHRR based aerosol climatology will be the lack of in situ aerosol optical depth information for the pre-AERONET era prior to 1993. This problem could be addressed in a similar manner like climate reconstructions. One half of the validation data is used to establish an appropriate processing scheme and the second half can independently assess the quality. If this quality assessment provides useful results, the applied processing scheme could be extended to the pre-AERONET era.

The purpose of this study is to point to a possible aerosol retrieval method eventually capable to produce an AVHRR based aerosol climatology. To achieve this goal further investigations are necessary, e.g. concerning different NOAA satellites, single scattering albedo or increased background aerosol load due to volcanic eruptions.

Acknowledgments. The authors are grateful to Alexander Ignatov for his very valuable remarks and comments. Thanks to Gerard Dedieu for providing the SMAC radiation transfer code. We would like to thank MeteoSwiss as well as the National Center for Environmental Prediction (NCEP) for supplying meteorological data. Additionally, we thank the AERONET PIs and their staff for establishing and maintaining the sites used in this study. This study has been funded by the Swiss Defense Procurement Agency. Support by the Stiftung Marchese Francesco Medici del Vascello is gratefully acknowledged.

References

- Ångström, A. (1961), Techniques of determining the turbidity of the atmosphere, *Tellus*, *XIII*, 214–223.
- Bertrand, C., and A. Royer (2004), Aerosol optical depth spatio-temporal characterization over the canadian boreas domain, *Int. J. Remote Sens.*, *25*(15), 2903–2917, doi:10.1080/01431160310001632657.
- Betts, A. K., and J. H. Ball (1997), Albedo over the boreal forest, *J. Geophys. Res.*, *102*(D24), 28,901–28,909.
- Borde, R., and J. Verdebout (2003), Remote sensing of aerosols optical thickness over various sites using SeaWiFS or VEGETATION and ground measurements, *Remote Sens. Environ.*, *86*(1), 42–51.
- Borde, R., D. Ramon, C. Schmechtig, and R. Santer (2003), Extension of the DDV concept to retrieve aerosol properties over land from the Modular Optoelectronic Scanner (MOS) sensor, *Int. J. Remote Sens.*, *24*(7), 1439–1467.
- Chu, D. A., Y. J. Kaufman, C. Ichoku, L. A. Remer, D. Tanré, and B. N. Holben (2002), Validation of MODIS aerosol optical depth retrieval over land, *Geophys. Res. Lett.*, *29*(12), 1617, doi:10.1029/2001GL013205.
- Chu, D. A., Y. J. Kaufman, G. Zibordi, J. D. Chern, J. Mao, C. Li, and B. N. Holben (2003), Global monitoring of air pollution over land from the earth observing system-terra moderate resolution imaging spectroradiometer (MODIS), *J. Geophys. Res.*, *108*(D21), 4661, doi:10.1029/2002JD003179.
- D’Almeida, G., P. Koepke, and E. Shettle (1991), Atmospheric aerosols: Global climatology and radiative characteristics, *A. Deepak, Hampton, Va, USA*, p. 561 pp.

- Di Vittorio, A. V., and W. J. Emery (2002), An automated, dynamic threshold cloud-masking algorithm for daytime AVHRR images over land, *IEEE Trans. on Geos. and Remote Sens.*, *40*(8), 1682–1694.
- Dubovik, O., A. Smirnov, B. N. Holben, M. D. King, Y. J. Kaufman, T. F. Eck, and I. Slutsker (2000), Accuracy assessments of aerosol optical properties retrieved from Aerosol Robotic Network (AERONET) Sun and sky radiance measurements, *J. Geophys. Res.*, *105*(D8), 9791–9806.
- Geogdzhayev, I. V., M. I. Mishchenko, W. B. Rossow, B. Cairns, and A. A. Lacis (2002), Global two-channel AVHRR retrievals of aerosol properties over the ocean for the period of NOAA-9 observations and preliminary retrievals using NOAA-7 and NOAA-11 data, *J. Atmos. Sci.*, *59*(3), 262–278.
- Goodrum, G., K. B. Kidwell, and W. Winston (2000), NOAA KLM user’s guide, <http://www2.ncdc.noaa.gov/docs/klm/>, National Environmental Satellite, Data, and Information Services (NESDIS).
- Higurashi, A., T. Nakajima, B. N. Holben, A. Smirnov, R. Frouin, and B. Chatenet (1999), A study of global aerosol optical climatology with two-channel AVHRR remote sensing, *J. Clim.*, *13*(12), 2011–2027.
- Holben, B. N., et al. (1998), AERONET—A federated instrument network and data archive for aerosol characterization, *Remote Sens. Environ.*, *66*, 1–16.
- Holzer-Popp, T., M. Schroedter, and G. Gesell (2002a), Retrieving aerosol optical depth and type in the boundary layer over land and ocean from simultaneous GOME spectrometer and ATSR-2 radiometer measurements, 1.Method description, *J. Geophys. Res.*, *107*(D21), 4578, doi:10.1029/2001JD002013.

- Holzer-Popp, T., M. Schroedter, and G. Gesell (2002b), Retrieving aerosol optical depth and type in the boundary layer over land and ocean from simultaneous GOME spectrometer and ATSR-2 radiometer measurements, 2. Case study application and validation, *J. Geophys. Res.*, *107*(D24), 4770, doi:10.1029/2002JD002777.
- Husar, R., J. Prospero, and L. Stowe (1997), Characterization of tropospheric aerosols over the oceans with the NOAA Advanced Very High Resolution Radiometer optical thickness operational product, *J. Geophys. Res.*, *102*(D14), 16,889–16,909.
- Ignatov, A. (2002), Sensitivity and information content of aerosol retrievals from Advanced Very High Resolution Radiometer: Radiometric factors, *Appl. Opt.*, *41*(6), 991–1011.
- Ignatov, A., and N. R. Nalli (2002), Aerosol retrievals from multi-year multi-satellite AVHRR pathfinder atmosphere (PATMOS) dataset for correcting remotely sensed sea surface temperatures, *J. Atmos. Oceanic Technol.*, *19*(12), 1986–2008.
- Ignatov, A., and L. Stowe (2000), Physical basis, premises, and self-consistency checks of aerosol retrievals from TRMM/VIRS, *J. Appl. Meteorol.*, *39*(12), 2259–2277.
- Ignatov, A., and L. Stowe (2002a), Aerosol retrievals from individual AVHRR channels. Part I: Retrieval algorithm and transition from Dave to 6S radiative transfer model, *J. Atmos. Sci.*, *59*(3), 313–334.
- Ignatov, A., and L. Stowe (2002b), Aerosol retrievals from individual AVHRR channels. Part II: Quality control, probability distribution functions, information content, and consistency checks of retrievals, *J. Atmos. Sci.*, *59*(3), 335–362.
- Ignatov, A., J. Sapper, S. Cox, I. Laszlo, N. R. Nalli, and K. B. Kidwell (2004), Operational aerosol observations (AEROBS) from AVHRR/3 on board NOAA-KLM satellites, *J. Atmos. Oceanic Technol.*, *21*(1), 3–26.

- Ignatov, A. M., L. L. Stowe, S. M. Sakerin, and G. K. Korotaev (1995), Validation of the NOAA/NESDIS satellite aerosol product over the North Atlantic in 1989, *J. Geophys. Res.*, *100*(D3), 5123–5132.
- IPCC (1995), *Climate Change 1995: The Science of Climate Change. Contribution of Working Group I to the Second Assessment of the Intergovernmental Panel on Climate Change*, Cambridge University Press, UK.
- IPCC (2001), *Climate Change 2001: The scientific basis. Contribution of Working Group I to the Third Assessment of the Intergovernmental Panel on Climate Change*, Cambridge University Press, Cambridge.
- Kaufman, Y., D. Tanre, L. A. Remer, E. F. Vermote, A. Chu, and B. N. Holben (1997a), Operational remote sensing of tropospheric aerosol over land from EOS moderate resolution imaging spectroradiometer, *J. Geophys. Res.*, *102*(D14), 17,051–17,067.
- Kaufman, Y. J. (1987), Satellite sensing of aerosol absorption, *J. Geophys. Res.*, *92*(D4), 4307–4617.
- Kaufman, Y. J., and C. Sendra (1988), Algorithm for automatic atmospheric corrections to visible and near-ir satellite imagery, *Int. J. Remote Sens.*, *9*(8), 1357–1381.
- Kaufman, Y. J., A. Wald, L. A. Remer, B.-C. Gao, R. R. Li, and L. Flynn (1997b), The MODIS 2.1-micron channel - correlation with visible reflectance for use in remote sensing of aerosols, *IEEE Trans. on Geos. and Remote Sens.*, *35*(5), 1286–1298.
- Key, J. (2002), The cloud and surface parameter retrieval (CASPR) system for polar AVHRR - user's guide, <http://stratus.ssec.wisc.edu>, Cooperative Institute for Meteorological Satellite Studies, University of Wisconsin, 1225 West Dayton St., Madison, WI 53562.

- King, M., D. M. Byrne, J. A. Reagan, and B. M. Herman (1980), Spectral variation of aerosol optical depth at Tucson, Arizona, between august 1975 and december 1977, *J. Appl. Meteorol.*, *19*, 723–732.
- King, M. D., Y. J. Kaufman, D. Tanré, and T. Nakajima (1999), Remote sensing of tropospheric aerosols from space: Past, present, and future, *Bull. Am. Meteorol. Soc.*, *80*(11), 2229–2259.
- Knapp, K. R., and L. L. Stowe (2002), Evaluating the potential for retrieving aerosol optical depth over land from AVHRR pathfinder atmosphere data, *J. Atmos. Sci.*, *59*(3), 279–293.
- Mishchenko, M. I., I. V. Geogdzhayev, B. Cairns, W. B. Rossow, and A. A. Lacis (1999), Aerosol retrievals over the ocean by use of channels 1 and 2 AVHRR data: sensitivity analysis and preliminary results, *Appl. Opt.*, *38*(36), 7325–7341.
- Mitchell, R. M. (1999), Calibration status of NOAA AVHRR solar reflectance channels: CalWatch revision 1, *Atmospheric Research Technical Paper 42*, CSIRO.
- Mitchell, R. M. (2001), In-flight characteristics of the space count of NOAA AVHRR channels 1 and 2, *Atmospheric Research Technical Paper 52*, CSIRO.
- Molineaux, B., A. Royer, and N. O’Neill (1998), Retrieval of Pinatubo aerosol optical depth and surface bidirectional reflectance from six years of AVHRR global vegetation index data over boreal forest, *J. Geophys. Res.*, *103*(D2), 1847–1856.
- Rahman, H., and G. Dedieu (1994), SMAC: a simplified method for the atmospheric correction of satellite measurements in the solar spectrum, *Int. J. Remote Sens.*, *15*(1), 123–143.

- Remer, L. A., A. E. Wald, and Y. J. Kaufman (2001), Angular and seasonal variation of spectral surface reflectance ratios: Implications for the remote sensing of aerosol over land, *IEEE Trans. on Geos. and Remote Sens.*, *39*(2), 275–283.
- Simpson, J. J., and J. R. Stitt (1998), A procedure for the detection and removal of cloud shadow from AVHRR data over land, *IEEE Trans. on Geos. and Remote Sens.*, *36*(3), 880–897.
- Soufflet, V., D. Tanré, A. Royer, and N. T. O’Neill (1997), Remote sensing of aerosols over boreal forest and lake water from AVHRR data, *Remote Sens. Environ.*, *60*, 22–34.
- Stowe, L., A. Ignatov, and R. Singh (1997), Development, validation, and potential enhancements to the second-generation operational aerosol product at the National Environmental Satellite, Data, and Information Service of the National Oceanic and Atmospheric Administration, *J. Geophys. Res.*, *102*(D14), 16,923–16,934.
- Tanré, D., C. Deroo, P. Duhaut, M. Herman, J. Morcrette, J. Perbos, and P. Deschamps (1990), Description of a computer code to simulate the satellite signal in the solar spectrum: the 5S code, *Int. J. Remote Sens.*, *11*(4), 659–668.
- Vermote, E., D. Tanré, and J.-J. Morcrette (1997), Second simulation of the satellite signal in the solar spectrum, 6S: An overview, *IEEE Trans. on Geos. and Remote Sens.*, *35*(3), 675–686.
- Von Hoyningen-Huene, W., M. Freitag, and J. B. Burrows (2003), Retrieval of aerosol optical thickness over land surfaces from top-of-atmosphere radiance, *J. Geophys. Res.*, *108*(D9), 4260, doi:10.1029/2001JD002018.
- Zhao, T. X.-P., L. L. Stowe, A. Smirnov, D. Crosby, J. Sapper, and C. R. McClain (2002), Development of a global validation package for satellite oceanic aerosol optical thick-

ness retrieval based on AERONET observations and its application to NOAA/NESDIS operational aerosol retrievals, *J. Atmos. Sci.*, *59*, 294–312.

Zhao, T. X.-P., I. Laszlo, B. N. Holben, C. Pietras, and K. J. Voss (2003), Validation of two-channel VIRS retrievals of aerosol optical thickness over ocean and quantitative evaluation of the impact from potential subpixel cloud contamination and surface wind effect, *J. Geophys. Res.*, *108*(D3), 4106, doi:10.1029/2002JD002346.

Zhao, T. X.-P., O. Dubovik, A. Smirnov, B. N. Holben, J. Sapper, C. Pietras, K. J. Voss, and R. Frouin (2004), Regional evaluation of an Advanced Very High Resolution Radiometer (AVHRR) two-channel aerosol retrieval algorithm, *J. Geophys. Res.*, *109*(D02204), doi:10.1029/2003JD003817.

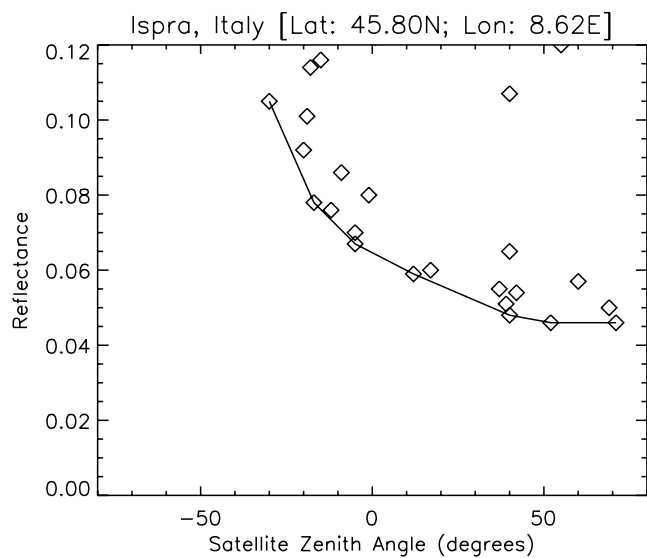


Figure 1. NOAA-16 AVHRR reflectance in channel 1 ($0.63\mu\text{m}$) for the period November 17, 2001 to December 31, 2001. Positive satellite zenith angles refer to forward scattering.

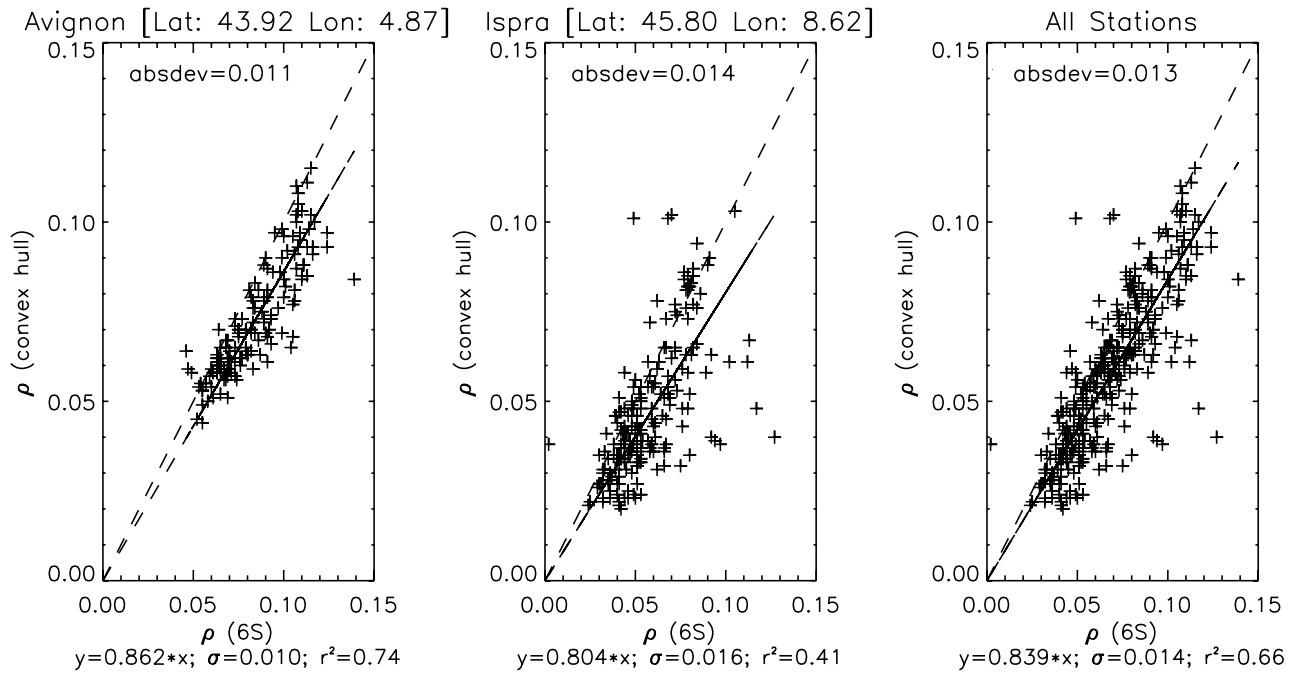


Figure 2. Scatter plot between NOAA-16 AVHRR retrieved surface reflectance ($\rho(\text{convex hull})$) and the modeled signal corrected with 6S and AERONET data ($\rho(6S)$). The 1:1 line is plotted as a dashed line, the linear fit as a solid line.

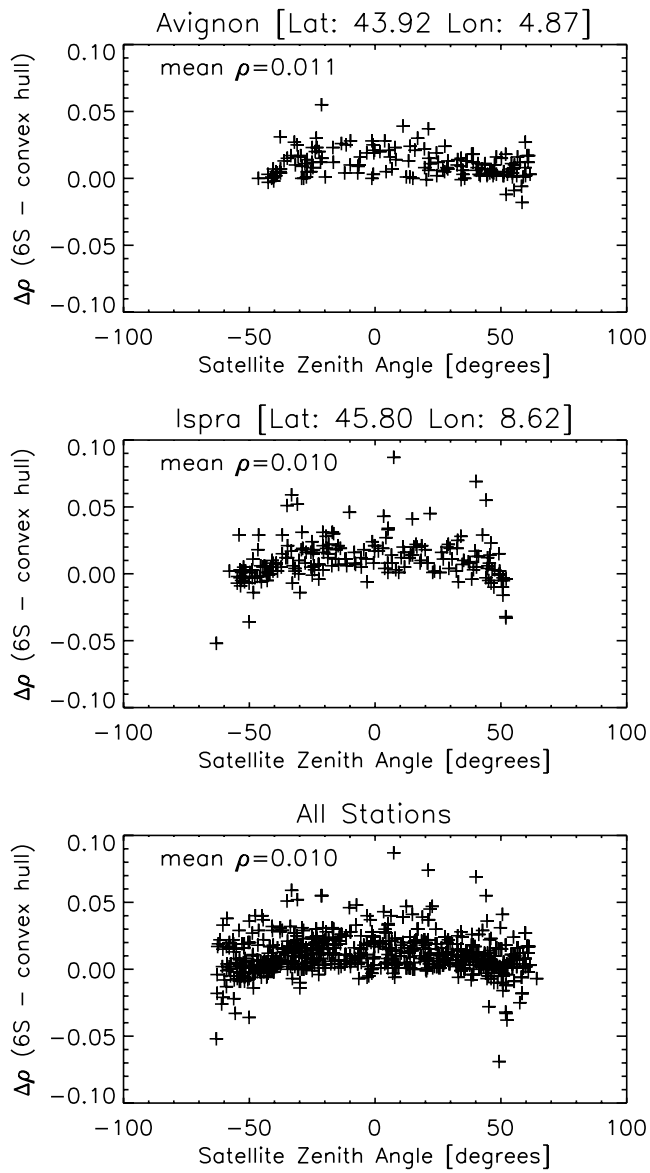


Figure 3. Difference between NOAA-16 AVHRR retrieved surface reflectance and 6S modeled data ($\Delta\rho(6S - \text{convex hull})$) plotted against the satellite zenith angle.

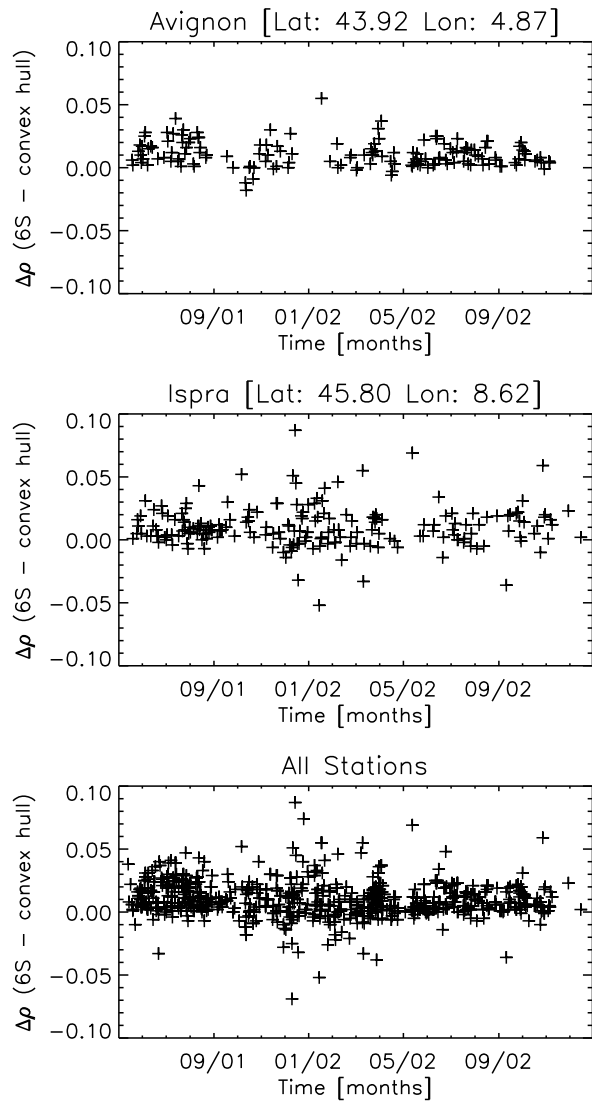


Figure 4. Time series of the difference between NOAA-16 AVHRR retrieved surface reflectance and 6S modeled data ($\Delta\rho(6S - \text{convex hull})$).

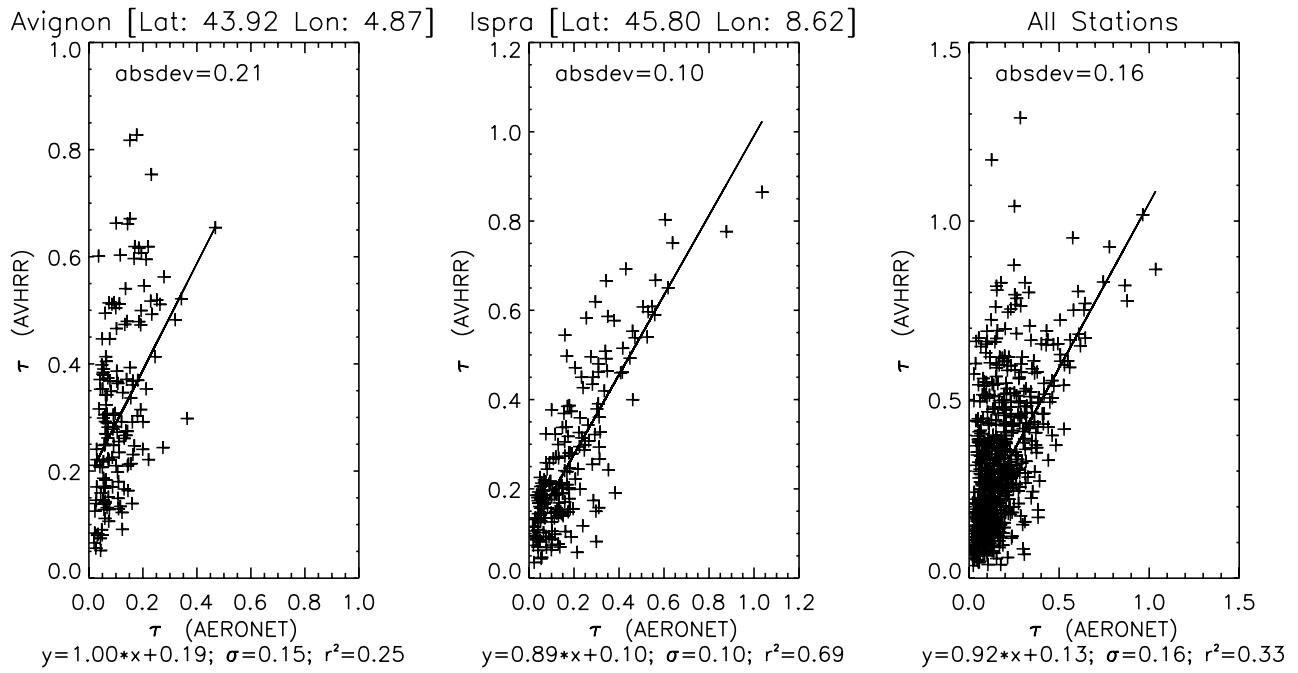


Figure 5. NOAA-16 AVHRR retrieved aerosol optical depth ($\tau(\text{AVHRR})$) from channel 1 ($0.63\mu\text{m}$) for the period May 2001 till December 2002 plotted against the AERONET aerosol optical depth ($\tau(\text{AERONET})$).

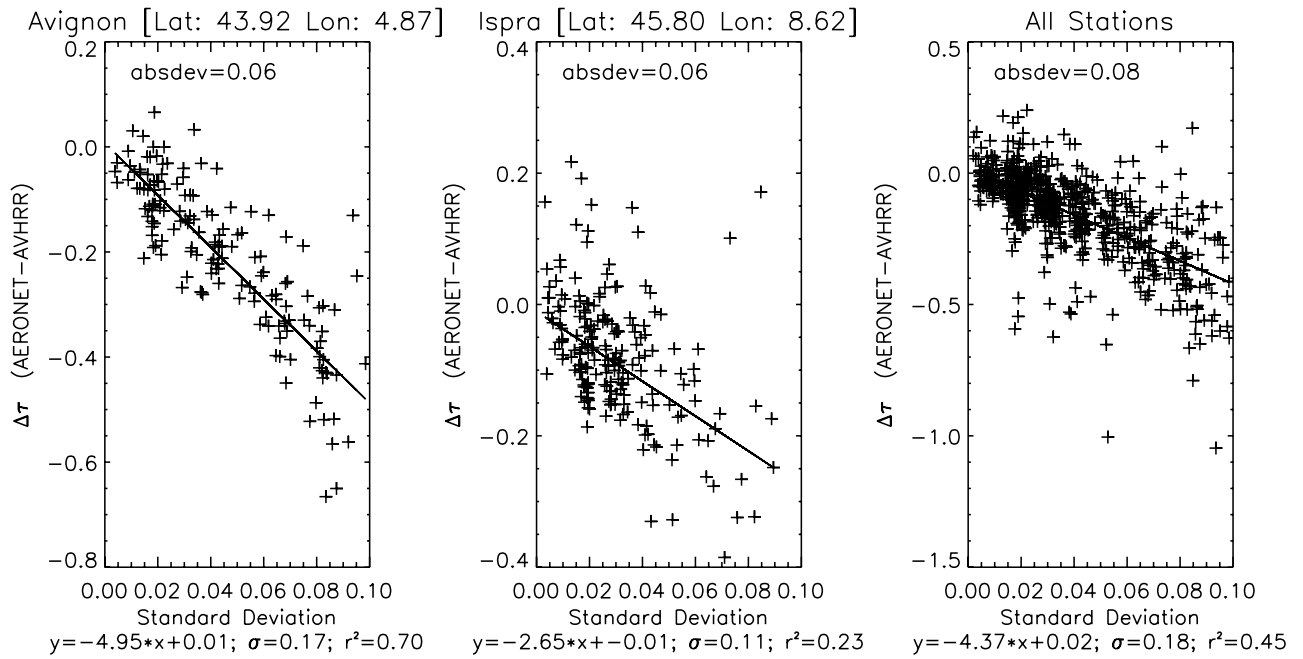


Figure 6. Aerosol optical depth (AOD) difference between AVHRR and AERONET ($\Delta\tau(\text{AERONET} - \text{AVHRR})$) plotted against the standard deviation of the AVHRR AOD inside a 25×25 pixel region around AERONET stations.

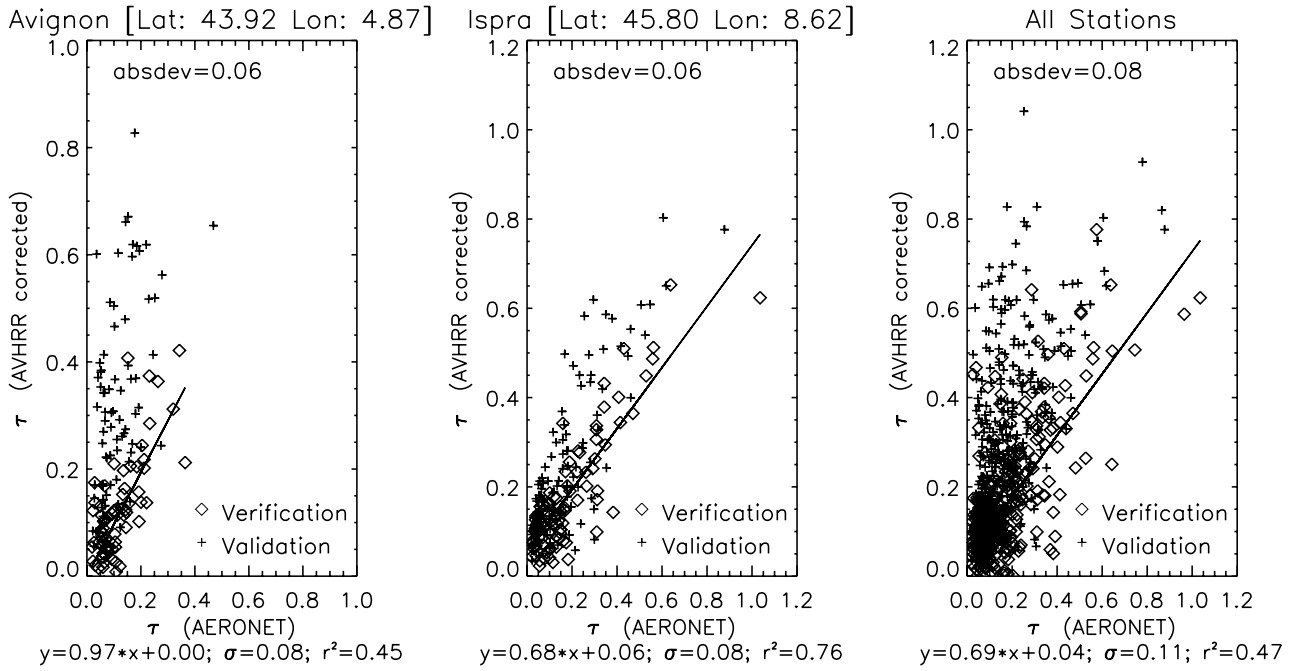


Figure 7. Scatter diagram between AVHRR aerosol optical depth (τ (AVHRR corrected)) and AERONET data (τ (AERONET)). The initial dataset used in figure 5 was split into two equal dataset, the validation dataset (plus) and the verification dataset (diamonds). The validation dataset is used to assess the linear fit like in figure 6 and tested on the verification dataset.

Table 1. Location of AERONET stations used in this study providing level 2 data and number of AVHRR-AERONET matchups (total: 678).

AERONET Site	Latitude	Longitude	Altitude (masl)	Matchups
Avignon	43°55'N	4°52'E	32	156
Creteil	48°47'N	2°26'E	57	-
Fontainebleu	48°24'N	2°40'E	85	23
Gerlitz	46°40'N	13°54'E	1900	-
Ispra	45°48'N	8°37'E	235	200
Marseille	43°16'N	5°23'E	100	18
Modena	44°37'N	10°56'E	56	46
Munich Maisach	48°12'N	11°15'E	520	21
Munich University	48°34'N	11°34'E	533	8
Rome Tor Vergata	41°50'N	12°38'E	130	123
Venice	45°18'N	12°30'E	10	83